Podophyllotoxin reduces the aggressiveness of human oral squamous cell carcinoma through myeloid cell leukemia-1

HYUN-JU YU, JI-AE SHIN, SU-JUNG CHOI and SUNG-DAE CHO

Department of Oral Pathology, School of Dentistry and Dental Research Institute, Seoul National University, Seoul 03080, Republic of Korea

Received May 18, 2023; Accepted September 5, 2023

DOI: 10.3892/ijmm.2023.5306

Abstract. Podophyllotoxin (PPT), which is derived from the podophyllum plant, exhibits marked cytotoxic effects against cancer cells; however, the precise molecular mechanism underlying its activity against human oral squamous cell carcinoma (OSCC) has not been elucidated. In the present study, the mechanism by which PPT induced cytotoxicity in two OSCC cell lines, HSC3 and HSC4, was determined. The effects of PPT on cytotoxicity in HSC3 and HSC4 cells were analyzed using Annexin V/PI double staining, Sub-G_1 analysis, soft agar assays, western blotting, and quantitative PCR. The changes in the mitochondrial membrane potential were assessed using a JC-1 assay and cytosolic and mitochondrial fractionation. A myeloid cell leukemia-1 (Mcl-1) overexpression cell lines were also established to study the role of Mcl-1 on apoptosis. The results showed that PPT inhibited the growth of the two human OSCC cell lines and induced apoptosis, which was accompanied by mitochondrial membrane depolarization. Compared with the control, PPT reduced the expression of Mcl-1 in both cell lines through a proteasome-dependent protein degradation process. Overall, these results suggested that targeting of Mcl-1 protein by PPT induced apoptosis, providing a foundation for further pre-clinical and clinical study of its value in the management of OSCC.

Introduction

Head and neck cancers are among the top seven most prevalent cancer types worldwide, of which, the majority (90%) are squamous cell carcinoma (1). There are several risk factors associated with the development of this cancer type, including premalignant conditions such as consumption of tobacco, betel nut, and alcohol, poor oral hygiene, UV radiation exposure, Epstein Barr virus infection, and human papillomavirus (HPV) infection (2,3). Oral cancer is a subtype of head and neck cancer that affects various oral mucosal regions, including the anterior two-thirds of the tongue, the gingival tissue, the mucosal lining of the lips and cheeks, the sublingual floor, the hard palate, and the retromolar region (4,5). Although significant progress has been made in oral cancer treatment, further studies are required to understand the mechanism of action of the therapeutic agents commonly used and the heterogeneous nature of this disease.

Podophyllotoxin (PPT) is a naturally occurring arylnaphthalene class of lignans found in the plants of the Podophyllum genus, such as *Podophyllum peltatum* and *Podophyllum emodi* (6). It is a folk remedy that exhibits antiproliferative properties similar to colchicine (7). PPT and its derivatives exhibit significant anticancer activity by destabilizing microtubules, which are structural elements of the cytoskeleton (8-10). PPT also exerts a broad range of highly effective antiviral and antibacterial properties (11). In 1990, the WHO recommended 0.5% PPT as a first-line drug for the treatment of condyloma acuminatum, which is usually caused by HPV (12). Two semi-synthesized podophyllotoxin glycosyl derivatives, etoposide (VP-16) and teniposide (VM-26), were approved by the FDA in 1983 and 1992 for anticancer therapy (12). Etoposide is used in frontline cancer therapy against various cancer types, such as small-cell lung cancer and testicular cancer (13-16), whereas teniposide is primarily used for the treatment of acute lymphoblastic leukemia (17). With respect to the molecular mechanisms, PPT exhibits potent anticancer effects by inhibiting DNA topoisomerase II and tubulin, respectively, which cause cell cycle arrest and DNA damage (11). The remarkable anticancer properties of PPT have been extensively studied. Moreover, a variety of novel compounds have been tested and demonstrated to be effective at treating various neoplasms. PPT derivatives cause cell cycle arrest and apoptosis associated with Bcl-2 in hepatocellular carcinoma and lung cancer (18,19). In addition, the synthesis and evaluation of a hybrid combining podophyllotoxin and coumarin was studied and found to be associated with the AKT/mTOR pathway in oral cancer (20). However, studies determining the effectiveness of PPT in treating oral

Correspondence to: Professor Sung-Dae Cho or Dr Su-Jung Choi, Department of Oral Pathology, School of Dentistry and Dental Research Institute, Seoul National University, 101 Daehak-ro, Jongno-gu, Seoul 03080, Republic of Korea
E-mail: efiwdsc@snu.ac.kr
E-mail: anna47408@snu.ac.kr

Key words: podophyllotoxin, oral squamous cell carcinoma, apoptosis, myeloid cell leukemia-1, mitochondrial membrane potential, proteasomal degradation

squamous cell carcinoma (OSCC) (20) are less common compared with those in other tumor types.

To identify the potent anticancer mechanism of action of PPT in OSCC, apoptosis associated with the Bcl-2 family of proteins, particularly myeloid cell leukemia-1 (Mcl-1) was assessed. In OSCC, the Mcl-1 gene is commonly amplified and upregulated, which affects the clinical course and survival of patients with this disease (21-24). Mcl-1 is also upregulated and is associated with poor outcomes in other malignant tumors, such as hematologic malignancies (25), breast cancer (26,27), lung (28), and gastric cancer (29). Mcl-1 blocks the oligomerization of the pro-apoptotic Bcl-2 family members, Bax and Bak, which sequesters them to produce protein-permeable holes in the mitochondrial outer membrane (30-32). Finally, a reduction in Mcl-1 expression promotes cytochrome C release into the cytoplasm, which activates the caspase cascade and induces apoptosis (21). Based on these findings, targeting Mcl-1 may represent a promising approach for treating OSCC.

In the present study, the cytotoxic effects of PPT against OSCC cell lines were assessed. It was found that PPT induced apoptosis in OSCC cells by activating the mitochondrial pathway through the downregulation of Mcl-1 at the post-translational level.

Materials and methods

Cell culture and reagents. The OSCC cell lines (HSC3 and HSC4) were obtained from Hokkaido University (Hokkaido, Japan) and cultured in DMEM/F12 medium (Welgene, Inc.) supplemented with 10% FBS and 1% antibiotics [penicillin/streptomycin (P/S)] (Welgene, Inc.) at 37˚C in a 5% CO_2 incubator. The Yonsei University kindly provided the Immortalized human oral keratinocyte (IHOK) cells. KSF medium (Gibco; Thermo Fisher Scientific, Inc.) supplemented with BPE/EGFR was used for maintaining IHOK cells. All experiments were performed with cells cultured to 50-60% confluence. PPT and cycloheximide (CHX) were purchased from MilliporeSigma (cat. no. P4405) and MG132 was obtained from Santa Cruz Biotechnology Inc. All chemicals were dissolved in DMSO and stored at -20˚C.

Trypan blue exclusion assay. The trypan blue exclusion assay was used to determine the effect of PPT on cell viability. The OSCC cells ($1.8x10^5$/ml HSC3 cells or $2.8x10^5$/ml HSC4 cells) were seeded into 6-well plates and incubated with 100 nM PPT for 24 h, followed by staining with 0.4% trypan blue (Gibco; Thermo Fisher Scientific, Inc.). The viable cells were counted using a Corning® Cell counter. All experiments were performed independently three times with triplicate samples for each experiment.

CCK-8 cell proliferation assay. To assess cell proliferation, the cells were seeded into 96-well plates and incubated with 100 nM PPT for 24 h. Then, 10 μl CCK-8 solution (cat. no. CK04-500; Dojindo Molecular Technologies, Inc.) was added to each well, thoroughly mixed with the culture media, and incubated at 37˚C for 2 h. The optical density (OD) of each well was measured using a Chameleon microplate reader (Hidex) at 450 nm and the OD values are reported as the mean ± SD.

Soft colony formation agar assay. Basal Medium Eagle (BME) with sodium carbonate was dissolved in sterile distilled water to prepare a 2x BME solution, which was then purified using a 0.2 μM syringe filter. The bottom agar (0.5%) was prepared by mixing 2x BME, L-glutamine, gentamicin, PBS, FBS, and 1.25% agar. The wells were pre-coated with 3 ml per well along with 0.3% top agar. After curing at room temperature (RT) for 1 h, 200 μl culture medium was added every 3 days with DMSO and 100 nM PPT, and the cells were incubated at 37˚C for 10-14 days. Images of the colonies were randomly captured (4 images per well) under a bright field microscope (Olympus Corporation) at a 40x magnification. The number of colonies with varying diameters was determined using ImageJ version 1.53t (National Institutes of Health).

Sphere formation assay. Cells were cultured in a serum-free medium containing 25 ng/ml EGF (Gibco; Thermo Fisher Scientific, Inc.) and bFGF (Invitrogen; Thermo Fisher Scientific, Inc.), 0.01x N-2, B27 supplement (Gibco; Thermo Fisher Scientific, Inc.), and 1% P/S and were seeded into ultra-low attachment 6-well plates (Corning®, Inc.) at a density of $1x10^4$ of cells/well. A total of 7-10 days after seeding, images of the spheres were randomly captured using an inverted light microscope (x20 magnification; Nikon Corporation) and counted in ImageJ.

Cell cycle distribution analysis. After treatment with PPT, HSC3 and HSC4 cells were collected, resuspended, washed with PBS, and fixed in 70% ethanol overnight at -20˚C. The cells were incubated with 20 μg/ml propidium iodide solution (PI; cat. no. P4170, MilliporeSigma) and RNase A (20 μg/ml) for 15 min at 37˚C. Cell cycle distribution was determined using an LSRFortessa™ Cell Analyzer (BD Biosciences). A minimum of 10,000 cells were analyzed for each sample using BD FACSDIVA™ software 6.0 (BD Biosciences). The percentage of the sub-G_1 fraction was quantified using FlowJo version 9/10 (FlowJo LLC).

Annexin V/PI double staining. Apoptosis was assessed using a FITC-Annexin V Apoptosis Detection kit (BD Pharmingen) according to the manufacturer's instructions. The floating and attached cells were gathered, washed with ice-cold PBS twice, and spun down in a centrifuge (180 x g, 5 min, 4˚C). The cells were then resuspended in Annexin V binding buffer and treated with 3 μl Annexin V-FITC for 15 min at room temperature in the dark, followed by the addition of 1 μl PI. The cells were then transferred to a FACS tube and analyzed by flow cytometry. The Annexin V(+)/PI(-) staining of cells indicated early-stage apoptosis, while Annexin V(+)/PI(+) staining indicated late-stage apoptosis. The percentage of cells displaying Annexin V/PI staining was determined by analyzing a minimum of 10,000 cells. The flow cytometry data were reanalyzed using FlowJo software.

Western blot analysis. Total protein was isolated from cells using RIPA lysis buffer (MilliporeSigma) containing 1% phosphatase inhibitor (Thermo Fisher Scientific Inc.) and protease inhibitor cocktails (Roche Diagnostics, GmbH). The protein concentration of each sample was measured using a DC Protein Assay kit (Bio-Rad Laboratories, Inc.). The protein lysates,

containing around 30-50 μg protein, were normalized and then mixed with 5x protein sample buffer. The mixture was heated at 95˚C for 5 min, separated on 8, 12, or 15% SDS gels, resolved using SDS-PAGE, and then transferred to Immuno-Blot PVDF membranes (MilliporeSigma). The membranes were added to 5% skimmed milk in Tris-buffered saline with Tween20 at RT for 2 h for blocking non-specific binding and incubated with primary antibodies overnight at 4˚C. The membranes were incubated with horseradish peroxidase-conjugated secondary antibodies for 2 h and developed using a WestGlow™ PICO PLUS Chemiluminescent substrate (Biomax, Inc.). The immunoreactive bands were visualized using an ImageQuant™ LAS 500 (GE Healthcare Life Sciences) or x-ray film. Densitometry analysis of the western blots was performed using Image J version 1.51k (National Institutes of Health). The primary antibodies used were: Cleaved poly (ADP-ribose) polymerase (PARP) (cat. no. 9541, 1:1,000), Mcl-1 (cat. no. 5453, 1:1,000), Bcl-2 (cat. no. 2870, 1:1,000), and Bcl-xL (cat. no. 2764, 1:1,000), all from Cell Signaling Technology, Inc. β-actin (cat. no. sc-47778, 1:3,000) and α-tubulin (cat. no. sc-5286, 1:3,000) were obtained from Santa Cruz Biotechnology Inc. Cytochrome C (cat. no. BD556433, 1:3,000) and CoxIV (cat. no. ab16056, 1:3,000) antibodies were obtained from BD Biosciences and Abcam, respectively.

Mitochondrial membrane potential (MMP) assay. ΔΨm was measured by flow cytometry using the lipophilic fluorescent dye JC-1 and the MitoScreen kit (BD Pharmingen). After trypsinization, the cells were washed with PBS, and collected by centrifugation at 1,120 x g at 4˚C for 5 min. The cell pellets were resuspended in 1x JC-1 working solution and incubated at 37˚C for 30 min in the dark. After staining, the cells were rinsed with 1x assay buffer and spun down in a centrifuge at 3500 rpm for 5 min The supernatant was removed, and the cells were resuspended in 1x assay buffer. Subsequently, the cells were transferred to FACS tubes and analyzed with an LSRFortessa™ Cell Analyzer. The proportion of stained cells was quantified using 10,000 cells per sample and analyzed using BD FACSDIVA™ software. The flow cytometry data were reanalyzed using FlowJo software.

Cytosolic and mitochondrial fractions. The isolation of the cytosolic and mitochondrial fractions was performed using the Mitochondria/Cytosol Fractionation Kit (Abcam). The procedure involved washing the cells with ice-cold PBS, spinning them down (4˚C for 5 min at 15,500 x g), and then resuspending the cell pellet in a mixture of 1x cytosol extraction buffer, DTT, and protease inhibitor for 10 min on ice. After centrifugation at 4˚C for 15 min at 15,500 x g, the supernatants, which contained cytosolic proteins, were collected and the pellets were resuspended in the mitochondrial extraction buffer. The supernatant containing the mitochondrial proteins was then obtained by another round of centrifugation (4˚C for 15 min at 15,500 x g).

Reverse transcription-quantitative PCR (RT-qPCR). The total RNA was extracted using TRIzol® Reagent. Then, 1 μg of the extracted RNA was reverse-transcribed using the AMPIGENE cDNA Synthesis kit (Enzo Life Sciences, Inc.) according to the manufacturer's protocol, and the resulting cDNA was subjected to qPCR using AMPIGENE qPCR Green Mix Hi-Rox (Enzo Life Sciences, Inc.). qPCR was performed using the Applied Biosystems StepOnePlus Real-Time PCR System with the following thermocycling conditions: 95˚C for 2 min; followed by 40 cycles of 95˚C for 10 sec and 60˚C for 30 sec. The relative expression levels of each gene were normalized to GAPDH and calculated using the $2^{-\Delta\Delta Cq}$ method (33). The sequences of the primers used are: Mcl-1 forward, 5'-GTATCA CAGACGTTCTCG-3', and reverse, 5'-AGAGGACCTAGA AGGTGG-3', and GAPDH forward, 5'-GTGGTCTCCTCT GACTTCAAC-3' and reverse, 5'-CCTGTTGCTGTAGCC AAATTC-3'.

Construction of the Mcl-1 overexpression vector and transient transfection. The pcDNA3.1-Mcl-1 overexpression vector was generated as described previously (32). HSC3 and HSC4 cells were treated with either 1 μg blank pcDNA3.1 vector or the pcDNA3.1-Mcl-1 vector using Lipofectamine® 2000 (Thermo Fisher Scientific, Inc.) for 12 h as per the manufacturer's guidelines.

Statistical analysis. Statistical analyses were performed using SPSS version 25.0 (IBM Corp.). A two-tailed Student's t-test was used for comparisons between two groups, and a one-way ANOVA followed by a Tukey's post-hoc test was used for comparisons between multiple groups. All graphs reflect the means and standard deviations of three separate experiments. $P<0.05$ was used to indicate a statistically significant difference.

Results

PPT inhibits the growth and colony formation of OSCC cell lines. To measure the cytotoxic effects of PPT on HSC3 and HSC4 cells, trypan blue exclusion and CCK-8 assays were performed following treatment with 100 nM PPT for 24 h. PPT significantly decreased the growth of both OSCC cell lines (Fig. 1A and B). To evaluate the effect of the PPT, the treatment period was extended from 48 to 72 h. This extended treatment revealed a sustained effect of PPT, confirming its prolonged efficacy (Fig. S1A). To ascertain the toxic effects on normal cell lines, IHOK cells were treated with 100 nM PPT for 24 h, and it was found that PPT did not affect the viability of the IHOK cells (Fig. S1B). To determine whether PPT influenced anchorage-independent growth in the HSC3 and HSC4 cell lines, soft agar assays were also performed by exposing the cell lines to PPT for 7-28 days. As evidenced by the size and quantity of the colonies, PPT significantly reduced the ability of cells to form colonies compared with the control (Fig. 1C). To explore the various facets of tumor behavior and drug response, spheroids were used as they are more capable of simulating cell-microenvironment interactions that closely mimic the 3D architecture of *in vivo* tumors. Notably, the results revealed the inhibition of spheroid formation upon PPT treatment (Fig. 1D). These results suggest that PPT inhibited malignant cancer cell growth in OSCC cell lines.

PPT increases the number of cells that undergo apoptosis in human OSCC cell lines. PPT treatment of cells led to cleavage of caspase3 and PARP, as revealed by western blot analysis. This suggests that PPT may induce apoptosis (Fig. 2A).

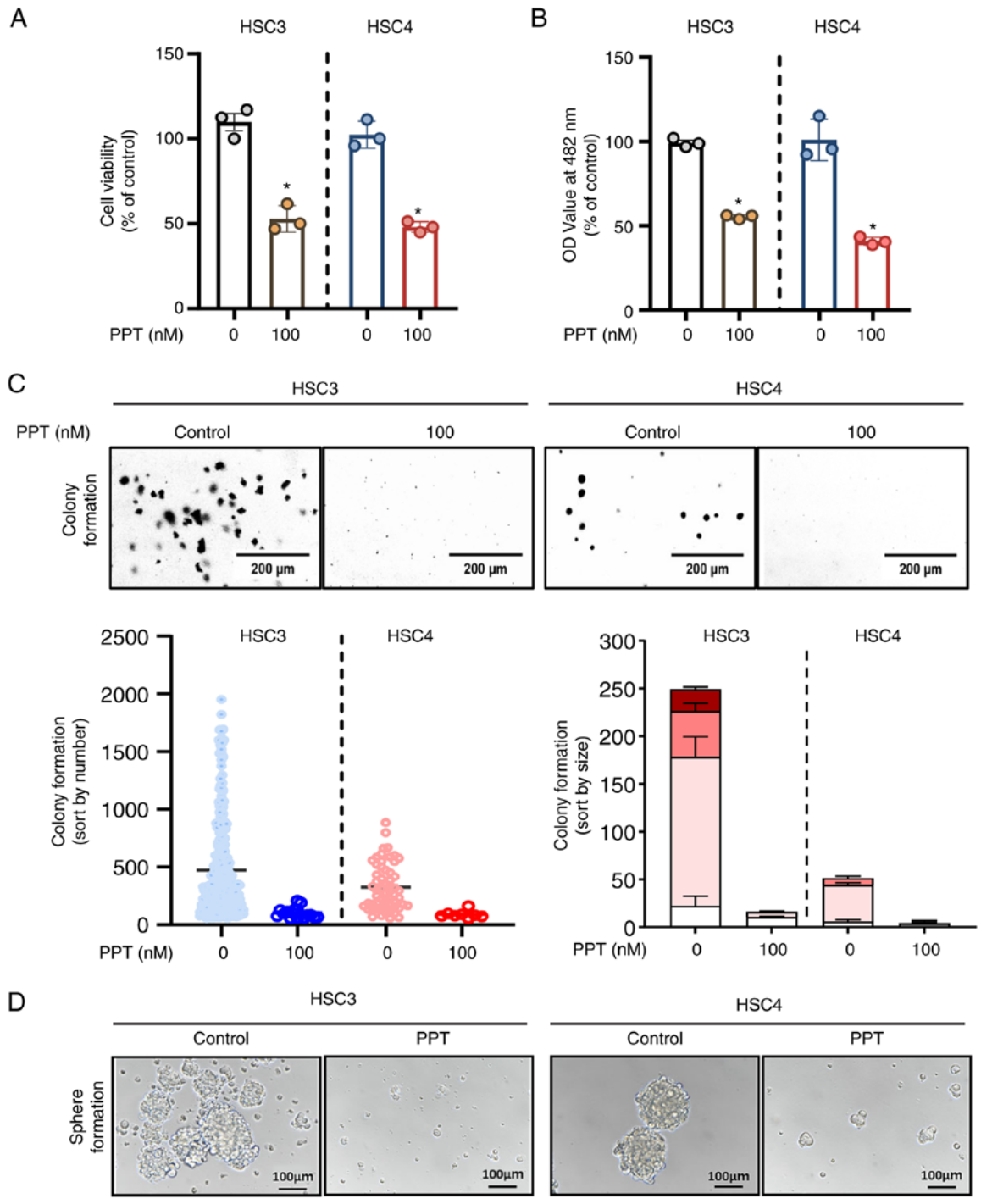

Figure 1. Effects of PPT on the survival of human OSCC cell lines. HSC3 and HSC4 cells were treated with DMSO or PPT for 24 h. (A) Cell viability was examined using an automated cell counter following treatment with DMSO or 100 nM PPT. (B) The cytotoxicity of PPT on both cell lines was measured using a CCK-8 assay. (C) A soft agar colony formation assay was used to evaluate anchorage-independent growth. (D) Representative images showing the sphere-formation efficiency in both HSC3 and HSC4 cell lines following treatment with DMSO or 100 nM PPT treatment. Scale bar, 100 μm. Data are presented as the mean ± SD of three independent experiments. *P<0.05. PPT, podophyllotoxin; OSCC, oral squamous cell carcinoma; OD, optical density.

Accordingly, a significant accumulation of apoptotic cells in the sub-G1 phase of the cell cycle was observed in PPT-treated cells (Fig. 2B). Flow cytometry analysis was performed to further evaluate the effect of PPT on apoptosis. This analysis provided information on the extent of cell death in response to PPT treatment. Compared with the solvent control, the percentage of Annexin V+ cells undergoing early-stage (Annexin V^+/PI^-) or late-stage (Annexin V^+/PI^+) apoptosis was increased following PPT treatment (Fig. 2C). Collectively, these results indicated that PPT induced apoptosis via a caspase-mediated pathway in human OSCC cell lines.

PPT influences the dysregulation of the MMP and the release of cytochrome C. To determine whether PPT-induced apoptosis in HSC3 and HSC4 cell lines was accompanied by mitochondrial dysfunction, the cationic dye JC-1 was used to detect changes in the MMP. Compared with the solvent control group, PPT treatment resulted in an increase in the monomeric

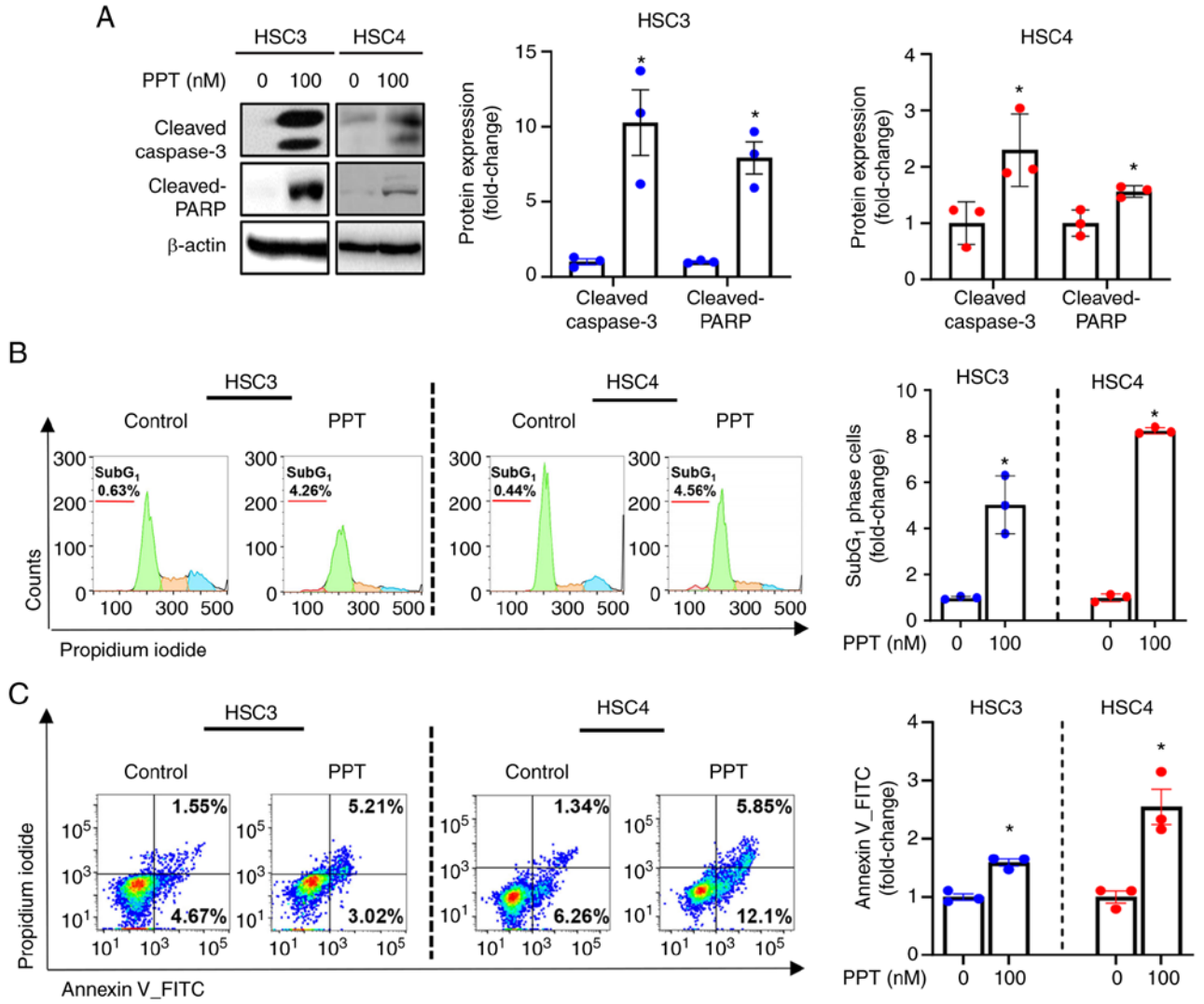

Figure 2. Effect of PPT on apoptosis of OSCC cells. (A) Western blot analysis of the expression of cleaved caspase3 and cleaved PARP. β-actin was used as the loading control. (B) The proportion of sub-G1 HSC3 and HSC4 cells following treatment with 100 nM PPT. (C) Annexin V/propidium iodide double staining was assessed using flow cytometry. Data are presented as the mean ± SD of three independent experiments. *P<0.05. PPT, podophyllotoxin; OSCC, oral squamous cell carcinoma; PARP, poly (ADP-ribose) polymerase.

form of JC-1, as indicated by an increase in cytosolic green fluorescence. This suggests that PPT may affect the MMP in cells (Fig. 3A). Furthermore, PPT induced the release of cytochrome C into the cytosol (Fig. 3B). Taken together, these results indicate that PPT promotes mitochondrial membrane depolarization and translocation of cytochrome C into the cytosol, which is considered an apoptotic event (34).

Downregulation of Mcl-1 protein by PPT is associated with post-translational modifications. To understand the mechanisms of mitochondrial membrane depolarization induced by PPT treatment, the expression of Bcl-2 family proteins (anti-apoptotic: Mcl-1, Bcl-2, Bcl-xL and pro-apoptotic: Bax, Bak) was evaluated. These proteins regulate the integrity of the mitochondria prior to apoptosis (34). The study aimed to identify the key molecules involved in the process. Significantly decreased Mcl-1 expression was observed in both cell lines following PPT treatment, whereas Bcl-2, Bcl-xL, Bax, and Bak were unchanged (Figs. 4A and S2). qPCR was performed to determine the effect of PPT on Mcl-1 mRNA levels. PPT had no obvious effects on Mcl-1 mRNA levels in either cell line (Fig. 4B). This suggested that Mcl-1 protein is regulated at the translational or post-translational level by PPT. To further assess whether PPT regulated the stability of Mcl-1, cells were treated with CHX to block new protein synthesis. Mcl-1 expression in the PPT and CHX-treated groups was reduced compared with the groups treated with CHX alone (Fig. 4C). The study found that pretreatment with MG132, a proteasome inhibitor, partially prevented the decrease in Mcl-1 expression caused by PPT treatment. This suggests that the proteasome pathway may play a role in the effects of PPT on Mcl-1 expression (Fig. 4D). Based on these findings, PPT contributed to a decrease in Mcl-1 protein levels through proteasome-mediated degradation. This suggests that the downregulation of Mcl-1 through proteasomal degradation is an important step in the death of human OSCC cell lines following PPT therapy.

Suppression of Mcl-1 following PPT treatment determines the susceptibility to apoptosis in human OSCC cell lines. The role of Mcl-1 in PPT-induced apoptosis was further investigated by

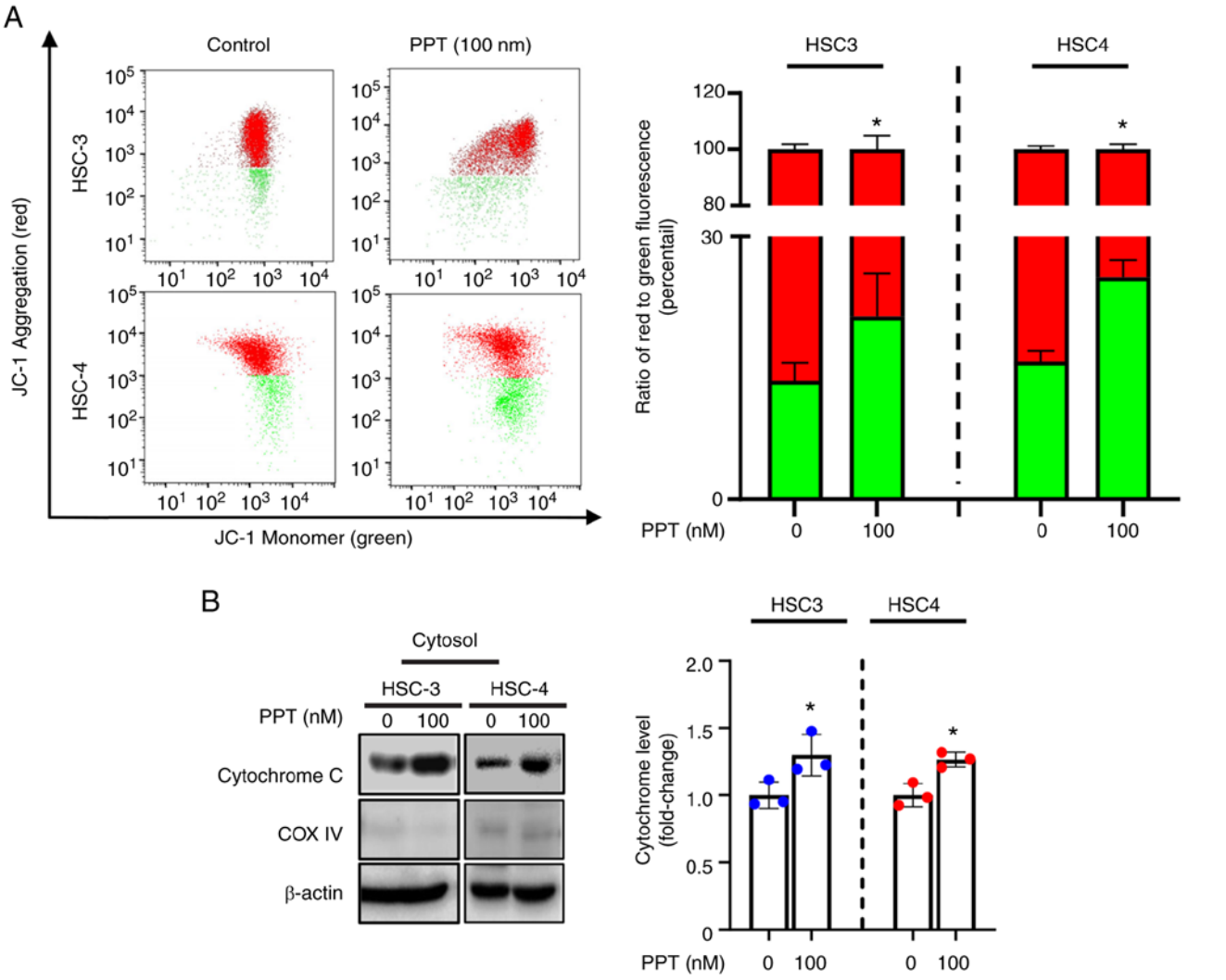

Figure 3. Effect of PPT on the mitochondrial membrane potential and the release of cytochrome C. (A) Measurement of the mitochondrial potential in OSCC cancer cells following treatment with PPT using a JC1 probe. (B) Cytochrome C release into the cytosol was assessed using a Mitochondria/Cytosol Fractionation Kit. Cox IV and β-actin were used as specific fraction markers for the mitochondria and cytosol, respectively. Western blots showing the expression of cytochrome C. β-actin was used as the internal control. Data are presented as the mean ± SD of three independent experiments. *P<0.05. PPT, podophyllotoxin; OSCC, oral squamous cell carcinoma.

overexpressing the Mcl-1 protein in human OSCC cell lines. This allowed for the study of the effect of increased Mcl-1 levels on the apoptotic response to PPT treatment. Compared with the vector control (pcDNA3.1), Mcl-1 overexpression (pcDNA3.1-Mcl-1) reduced the levels of cleaved caspase3 and cleaved PARP induced by PPT treatment (Fig. 5A). These data indicate that Mcl-1 acts as a determinant of PPT-induced apoptotic cell death in human OSCC cells. The suppressive effect of Mcl-1 in PPT-induced apoptosis was further established using flow cytometry analysis. The percentage of Annexin V-positive cell lines following PPT treatment was decreased following Mcl-1 overexpression (Fig. 5B). These findings indicated that Mcl-1 suppression may be necessary for PPT-induced apoptosis in human OSCC cell lines.

Discussion

Currently, it is very difficult to predict the disease progression of OSCC, given the anatomical complexities and varied pathological subtypes (3). Thus, studies are ongoing to address this issue by developing novel methods for the management of OSCC. Numerous anticancer strategies are focused on inducing or restoring apoptosis, which may inhibit cancer cell growth when apoptotic signaling pathways are reactivated (35). Indeed, growth inhibition through apoptosis induction using pharmacological approaches are established effective anticancer strategies in OSCC (23,36-39). In the present study, the growth of OSCC cells through induction of apoptosis using PPT was assessed. PPT treatment significantly reduced the growth of OSCC and inhibited anchorage-independent colony formation as determined using soft agar assays. Spheroid formation assays were used to better mimic the complex 3D structures of tumors *in vivo* (40). The ability of PPT on additional dimensions of tumor behavior and drug response in OSCC was assessed and the results showed that spheroid formation was inhibited when treated with PPT. In addition, PPT treatment markedly increased the levels of apoptotic indicators, such as cleaved-PARP, cleaved-caspase3, and Annexin V double staining. Recently, Bai *et al* (20) demonstrated that the novel

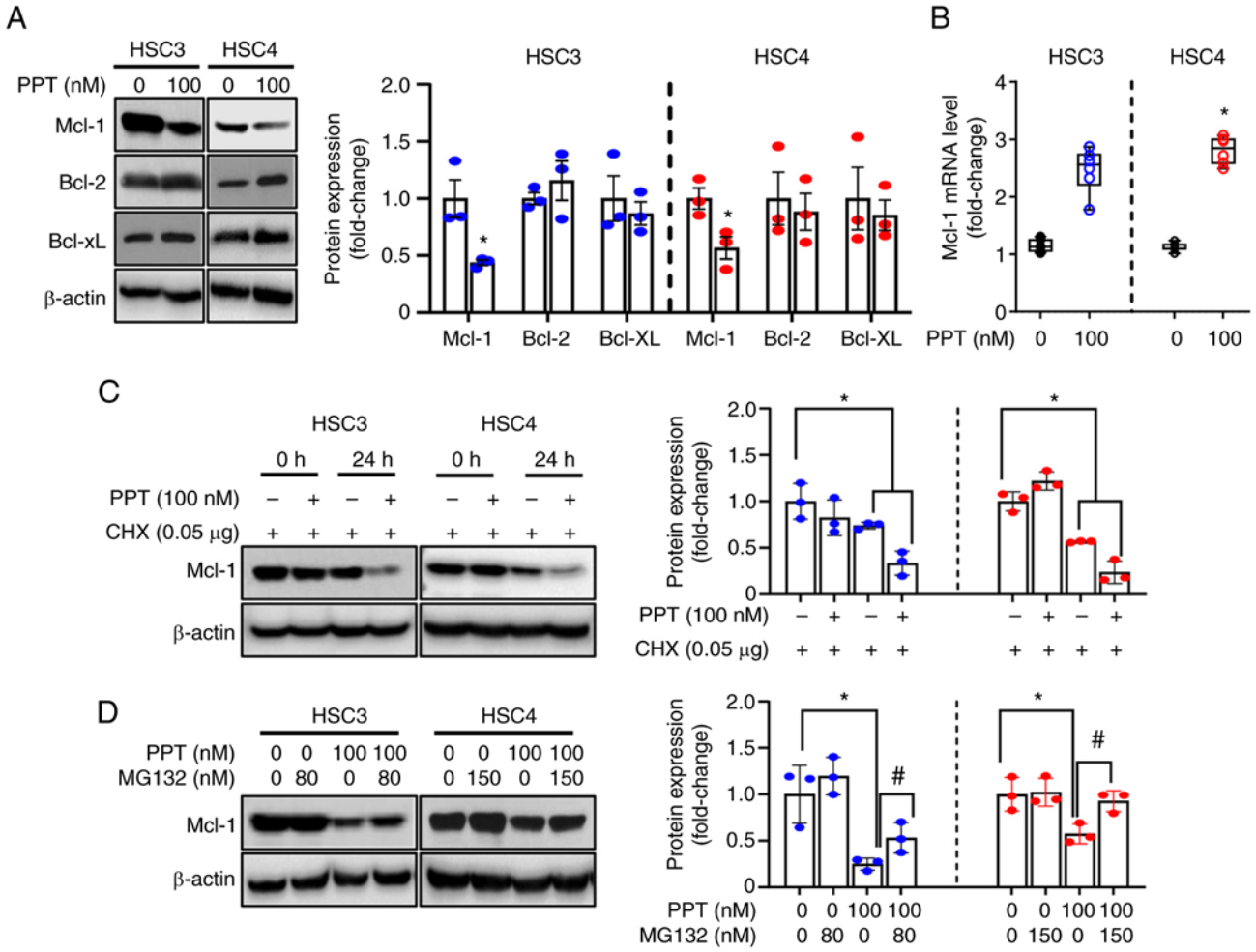

Figure 4. Effect of PPT on Mcl-1 protein turnover in human OSCC cell lines. (A) Western blots showing the expression of Mcl-1, Bcl-2, and Bcl-xL. (B) The expression levels of Mcl-1 in PPT-treated HSC3 and HSC4 cells were evaluated using quantitative PCR and were compared to the reference gene GAPDH to normalize the results. (C) Cells were pretreated with CHX or (D) MG132 for 1 h in the presence or absence of 100 nM PPT for 24 h, after which Mcl-1 protein expression was determined. Data are presented as the mean ± SD of three independent experiments. *P<0.05 compared with the control group; #P<0.05 compared with PPT-treated group. PPT, podophyllotoxin; OSCC, oral squamous cell carcinoma; Mcl-1, myeloid cell leukemia-1; CHX, Cycloheximide.

combination of PPT and coumarin exerted potent anti-cancer activity in OSCC via regulation of the AKT/mTOR pathway, supporting the results of the present study. Together, these suggest that PPT induces apoptosis, which in turn affects OSCC cell survival.

An important mechanism of several chemotherapeutic drugs is the disruption of normal tubulin function (41,42). PPT, a natural tubulin inhibitor, inhibits the growth of cancer cells by disrupting tubulin polymerization, which causes cell cycle arrest and inhibition of microtubule synthesis during the formation of mitotic spindles (43). Numerous studies have demonstrated the anticancer properties of PPT and its derivatives against various types of cancer by targeting different molecular targets (11,20,43,44). For example, PPT led to the production of reactive oxygen species and r-H2AX and activated the ATM/p53/p21 pathway to trigger DNA damage in human breast cancer (43). PPT also induced apoptosis in human lung cancer cells by inhibiting c-MET kinase activity (45). However, additional studies are still required to identify the anticancer mechanism of PPT in OSCC. OSCC cell lines exhibit significantly high expression of Mcl-1, which occurs through genetic amplification (21,46). As a commonly amplified and upregulated protein in OSCC malignant lesions, Mcl-1 promotes the development of cancer and reduces the survival of patients with cancer (21,47). As targeting Mcl-1 may be an important step in inducing programmed cell death, the use of natural compounds to attenuate Mcl-1 expression is considered a promising strategy for developing preventative and therapeutic regimens in OSCC (22,48). Previously, it was found that nitidine chloride, a naturally derived compound, decreased Mcl-1 protein expression by inhibiting the STAT3 pathway (23) and several natural products including *Sanguisorba officinalis* were found to reduce Mcl-1 expression via specificity protein 1 and thus induce apoptosis in OSCC cell lines (49,50). Fisetin also suppressed oral cancer growth by modulating the SESN2/mTOR/Mcl-1 signaling axis (39) suggesting that targeting Mcl-1 by PPT may be a promising treatment strategy for the management of OSCC. In the present study, whether PPT affected Mcl-1 protein in OSCC cell lines was assessed. PPT treatment specifically decreased Mcl-1 expression and Mcl-1 overexpression (pcDNA3.1-Mcl-1) restored PPT-induced apoptosis. Mcl-1 mRNA levels were unchanged following PPT treatment, which ruled out the possibility that PPT affected the transcriptional

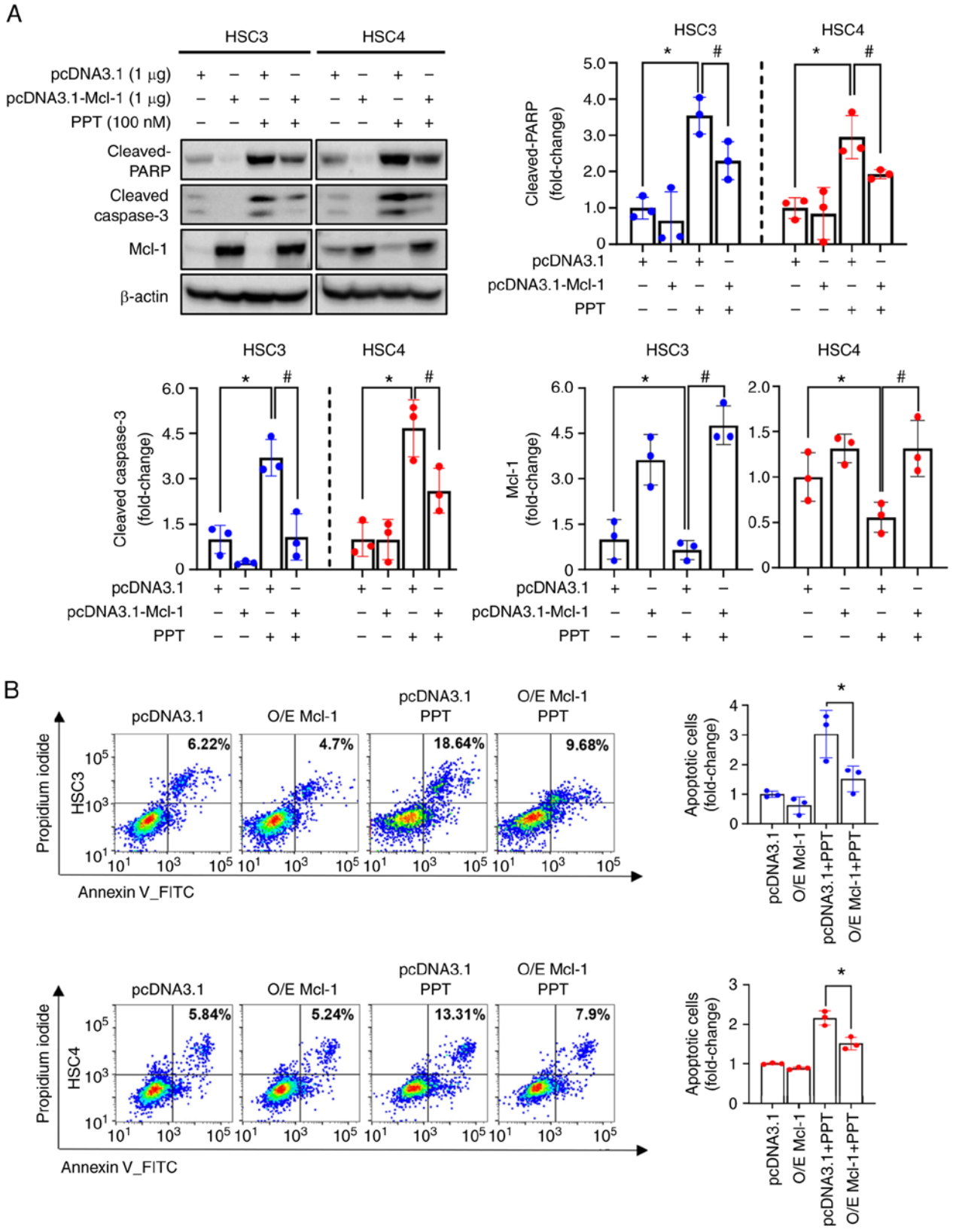

Figure 5. Rescue of PPT-mediated apoptosis by Mcl-1 overexpression in HSC3 and HSC4 cells. HSC3 and HSC4 cells were transiently transfected with 1 μg pcDNA3.1 or pcDNA3.1-Mcl-1-overexpression vector for 12 h and then treated with DMSO or 100 nM PPT for 24 h. (A) Western blots showing the expression of cleaved PARP, cleaved caspase3 and Mcl-1. *P<0.05 vs. control; $^{\#}$P<0.05 vs. PPT-treated group. (B) FACS analysis was used to quantify Annexin V/PI double staining. Data are presented as the mean ± SD of three independent experiments. PPT, podophyllotoxin; OSCC, oral squamous cell carcinoma; Mcl-1, myeloid cell leukemia-1; PARP, poly (ADP-ribose) polymerase.

regulation of Mcl-1. Numerous studies have demonstrated that decreased Mcl-1 expression, which may be caused by various compounds in cancer cells, is dependent on proteasomal processes (23,51). Thus, it is hypothesized that PPT induces

a rapid turnover of Mcl-1 protein in OSCC cell lines. In the present study, PPT affected Mcl-1 turnover, as evidenced based on the effects of the protein synthesis inhibitor and MG-132. These findings indicated that proteasome-dependent degradation, rather than transcriptional effects, was responsible for the observed PPT-induced Mcl-1 decrease in OSCC cell lines. Other studies have demonstrated that Mcl-1 is a key regulator for the apoptotic effects of anti-tubulin drugs, which cause a reduction in Mcl-1 protein at the post-translational level, to potentiate cell death (52,53), are consistent with the findings of the present study. Overall, these data suggested that Mcl-1 contributes to PPT-induced apoptotic cell death in OSCC cell lines such as other tubulin inhibitors or naturally derived compounds.

In conclusion, it was found that PPT triggers anti-tumor growth and colony formation in OSCC cell lines by inducing mitochondrial-dependent apoptosis. These results were associated with decreased expression of Mcl-1 at the protein level. Taken together, these findings suggest that PPT may serve as a potential novel therapeutic drug candidate for targeting Mcl-1 in OSCC.

Acknowledgements

Not applicable.

Funding

This work was supported by the National Research Foundation of Korea through a grant funded by the Korean government (MSIT) (grant no. 2022R1A2C1091608) and the Ministry of Education (grant no. 2019R1A2C1085896).

Availability of data and materials

The datasets used and/or analyzed during the present study are available from the corresponding author on reasonable request.

Authors' contributions

HJY and SJC conceived the study, acquired and analyzed the data, and drafted the manuscript. SJC and JAS analyzed and interpreted the data. SDC designed and interpreted the study. SJC and SDC reviewed and edited the manuscript, and participated in contributing to the contents of the revised manuscript. SJC and SDC confirm the authenticity of all the raw data.

Ethics approval and consent to participate

Not applicable.

Patient consent for publication

Not applicable.

Competing interests

The authors declare that they have no competing interests.

References

1. Sung H, Ferlay J, Siegel RL, Laversanne M, Soerjomataram I, Jemal A and Bray F: Global cancer statistics 2020: GLOBOCAN estimates of incidence and mortality worldwide for 36 cancers in 185 countries. CA Cancer J Clin 71: 209-249, 2021.
2. Hernandez BY, Zhu X, Goodman MT, Gatewood R, Mendiola P, Quinata K and Paulino YC: Betel nut chewing, oral premalignant lesions, and the oral microbiome. PLoS One 12: e0172196, 2017.
3. Usman S, Jamal A, The MT and Waseem A: Major molecular signaling pathways in oral cancer associated with therapeutic resistance. Front Oral Health 1: 603160, 2021.
4. Hanna GJ, Patel N, Tedla SG, Baugnon KL, Aiken A and Agrawal N: Personalizing surveillance in head and neck cancer. Am Soc Clin Oncol Educ Book 43: e389718, 2023.
5. Gormley M, Creaney G, Schache A, Ingarfield K and Conway DI: Reviewing the epidemiology of head and neck cancer: Definitions, trends and risk factors. Br Dent J 233: 780-786, 2022.
6. Xu H, Lv M and Tian X: A review on hemisynthesis, biosynthesis, biological activities, mode of action, and structure-activity relationship of podophyllotoxins: 2003-2007. Curr Med Chem 16: 327-349, 2009.
7. King ML and Sullivan MM: The similarity of the effect of podophyllin and colchicine and their use in the treatment of condylomata acuminata. Science 104: 244-245, 1946.
8. Desbène S and Giorgi-Renault S: Drugs that inhibit tubulin polymerization: The particular case of podophyllotoxin and analogues. Curr Med Chem Anticancer Agents 2: 71-90, 2002.
9. Chen SW, Wang YH, Jin Y, Tian X, Zheng YT, Luo DQ and Tu YQ: Synthesis and anti-HIV-1 activities of novel podophyllotoxin derivatives. Bioorg Med Chem Lett 17: 2091-2095, 2007.
10. Xu H and Xiao X: Natural products-based insecticidal agents 4. Semisynthesis and insecticidal activity of novel esters of 2-chloropodophyllotoxin against Mythimna separata Walker in vivo. Bioorg Med Chem Lett 19; 5415-5418, 2009.
11. Zhao W, Cong Y, Li HM, Li S, Shen Y, Qi Q, Zhang Y, Li YZ and Tang YJ: Challenges and potential for improving the druggability of podophyllotoxin-derived drugs in cancer chemotherapy. Nat Prod Rep 38: 470-488, 2021.
12. Paz-Ares L, Dvorkin M, Chen Y, Reinmuth N, Hotta K, Trukhin D, Statsenko G, Hochmair MJ, Özgüroğlu M, Ji JH, *et al*: Durvalumab plus platinum-etoposide versus platinum-etoposide in first-line treatment of extensive-stage small-cell lung cancer (CASPIAN): A randomised, controlled, open-label, phase 3 trial. Lancet 394: 1929-1939, 2019.
13. Conlon KC, Sportes C, Brechbiel MW, Fowler DH, Gress R, Miljkovic MD, Chen CC, Whatley MA, Bryant BR, Corcoran EM, *et al*: ^{90}Y-daclizumab (anti-CD25), high-dose carmustine, etoposide, cytarabine, and melphalan chemotherapy and autologous hematopoietic stem cell transplant yielded sustained complete remissions in 4 patients with recurrent Hodgkin's lymphoma. Cancer Biother Radiopharm 35: 249-261, 2020.
14. Tsukamoto Y, Kiyasu J, Choi I, Kozuru M, Uike N, Utsunomiya H, Hirata A, Fujioka E, Ohno H, Nakashima E, *et al*: Efficacy and safety of the modified EPOCH regimen (etoposide, vincristine, doxorubicin, carboplatin, and prednisolone) for adult T-cell leukemia/lymphoma: A multicenter retrospective study. Clin Lymphoma Myeloma Leuk 20: e445-e453, 2020.
15. Liang J, Bi N, Wu S, Chen M, Lv C, Zhao L, Shi A, Jiang W, Xu Y, Zhou Z, *et al*: Etoposide and cisplatin versus paclitaxel and carboplatin with concurrent thoracic radiotherapy in unresectable stage III non-small cell lung cancer: A multicenter randomized phase III trial. Ann Oncol 28: 777-783, 2017.
16. Manapov F and Eze C: Survival advantage for etoposide/cisplatin over paclitaxel/carboplatin concurrent chemoradiation in patients with inoperable stage III NSCLC: A subgroup analysis for ECOG 2 patients would be of great interest. Ann Oncol 28: 2319-2320, 2017.
17. Bugg BY, Danks MK, Beck WT and Suttle DP: Expression of a mutant DNA topoisomerase II in CCRF-CEM human leukemic cells selected for resistance to teniposide. Proc Natl Acad Sci USA 88: 7654-7658, 1991.
18. Kamal A, Nayak VL, Bagul C, Vishnuvardhan MV and Mallareddy A: Investigation of the mechanism and apoptotic pathway induced by 4β cinnamido linked podophyllotoxins against human lung cancer cells A549. Apoptosis 20: 1518-1529, 2015.
19. Wang Y, Sun H, Xiao Z, Zhang D, Bao X and Wei N: XWL-1-48 exerts antitumor activity via targeting topoisomerase II and enhancing degradation of Mdm2 in human hepatocellular carcinoma. Sci Rep 7: 9989, 2017.

20. Bai G, Zhao D, Ran X, Zhang L and Zhao D: Novel hybrids of podophyllotoxin and coumarin inhibit the growth and migration of human oral squamous carcinoma cells. Front Chem 8: 626075, 2021.
21. Choi SJ, Swarup N, Shin JA, Hong SD and Cho SD: Myeloid cell leukemia-1 expression in cancers of the oral cavity: A scoping review. Cancer Cell Int 22: 182, 2022.
22. Shin JA, Jung JY, Ryu MH, Safe S and Cho SD: Mithramycin A inhibits myeloid cell leukemia-1 to induce apoptosis in oral squamous cell carcinomas and tumor xenograft through activation of Bax and oligomerization. Mol Pharmacol 83: 33-41, 2013.
23. Yang IH, Jung W, Kim LH, Shin JA, Cho NP, Hong SD, Hong KO and Cho SD: Nitidine chloride represses Mcl-1 protein via lysosomal degradation in oral squamous cell carcinoma. J Oral Pathol Med 47: 823-829, 2018.
24. Jung M, Han DJ, Ahn CH, Hong KO, Choi YS, Kim JS, Yoon HJ, Hong SD, Shin JA and Cho SD: *In vitro* induction of mitotic catastrophe as a therapeutic approach for oral cancer using the ethanolic extract of Juniperus squamata. Oncol Rep 45: 103, 2021.
25. Wei AH, Roberts AW, Spencer A, Rosenberg AS, Siegel D, Walter RB, Caenepeel S, Hughes P, McIver Z, Mezzi K, *et al*: Targeting MCL-1 in hematologic malignancies: Rationale and progress. Blood Rev 44: 100672, 2020.
26. Campbell KJ, Dhayade S, Ferrari N, Sims AH, Johnson E, Mason SM, Dickson A, Ryan KM, Kalna G, Edwards J, *et al*: MCL-1 is a prognostic indicator and drug target in breast cancer. Cell Death Dis 9: 19, 2018.
27. Wein L and Loi S: Mechanisms of resistance of chemotherapy in early-stage triple negative breast cancer (TNBC). Breast 34 (Suppl 1): S27-S30, 2017.
28. Nakano T, Go T, Nakashima N, Liu D and Yokomise H: Overexpression of antiapoptotic MCL-1 predicts worse overall survival of patients with non-small cell lung cancer. Anticancer Res 40: 1007-1014, 2020.
29. Lee WS, Park YL, Kim N, Oh HH, Son DJ, Kim MY, Oak CY, Chung CY, Park HC, Kim JS, *et al*: Myeloid cell leukemia-1 is associated with tumor progression by inhibiting apoptosis and enhancing angiogenesis in colorectal cancer. Am J Cancer Res 5: 101-113, 2014.
30. Perciavalle RM and Opferman JT: Delving deeper: MCL-1's contributions to normal and cancer biology. Trends Cell Biol 23: 22-29, 2013.
31. Levine B, Sinha S and Kroemer G: Bcl-2 family members: Dual regulators of apoptosis and autophagy. Autophagy 4: 600-606, 2008.
32. Willis SN, Chen L, Dewson G, Wei A, Naik E, Fletcher JI, Adams JM and Huang DC: Proapoptotic Bak is sequestered by Mcl-1 and Bcl-xL, but not Bcl-2, until displaced by BH3-only proteins. Genes Dev 19: 1294-1305, 2005.
33. Livak KJ and Schmittgen TD: Analysis of relative gene expression data using real-time quantitative PCR and the 2(-Delta Delta C(T)) method. Methods 25: 402-408, 2001.
34. Wang C and Youle RJ: The role of mitochondria in apoptosis*. Annu Rev Genet 43: 95-118, 2009.
35. Wong RS: Apoptosis in cancer: From pathogenesis to treatment. J Exp Clin Cancer Res 30: 87, 2011.
36. Hsu S, Singh B and Schuster G: Induction of apoptosis in oral cancer cells: Agents and mechanisms for potential therapy and prevention. Oral Oncol 40: 461-473, 2004.
37. Yang IH, Hong SH, Jung M, Ahn CH, Yoon HJ, Hong SD, Cho SD and Shin JA: Cryptotanshinone chemosensitivity potentiation by TW-37 in human oral cancer cell lines by targeting STAT3-Mcl-1 signaling. Cancer Cell Int 20: 405, 2020.
38. Choi SJ, Ahn CH, Yang IH, Jin B, Lee WW, Kim JH, Ahn MH, Swarup N, Hong KO, Shin JA, *et al*: Pseudolaric acid B induces growth inhibition and caspase-dependent apoptosis on head and neck cancer cell lines through death receptor 5. Molecules 24: 3715, 2019.
39. Won DH, Chung SH, Shin JA, Hong KO, Yang IH, Yun JW and Cho SD: Induction of sestrin 2 is associated with fisetin-mediated apoptosis in human head and neck cancer cell lines. J Clin Biochem Nutr 64: 97-105, 2019.
40. Kapałczyńska M, Kolenda T, Przybyła W, Zajączkowska M, Teresiak A, Filas V, Ibbs M, Bliźniak R, Łuczewski Ł and Lamperska K: 2D and 3D cell cultures-a comparison of different types of cancer cell cultures. Arch Med Sci 14: 910-919, 2018.
41. Pang YQ, Lin H, Ou C, Cao Y, An B, Yan J and Li X: Design, synthesis, and biological evaluation of novel benzodiazepine derivatives as anticancer agents through inhibition of tubulin polymerization in vitro and in vivo. Eur J Med Chem 182: 111670, 2019.
42. Mukhtar E, Adhami VM and Mukhtar H: Targeting microtubules by natural agents for cancer therapy. Mol Cancer Ther 13: 275-284, 2014.
43. Zhang X, Rakesh KP, Shantharam CS, Manukumar HM, Asiri AM, Marwani HM and Qin HL: Podophyllotoxin derivatives as an excellent anticancer aspirant for future chemotherapy: A key current imminent needs. Bioorg Med Chem 26: 340-355, 2018.
44. Xiao J, Gao M, Sun Z, Diao Q, Wang P and Gao F: Recent advances of podophyllotoxin/epipodophyllotoxin hybrids in anticancer activity, mode of action, and structure-activity relationship: An update (2010-2020). Eur J Med Chem 208: 112830, 2020.
45. Chen JY, Tang YA, Li WS, Chiou YC, Shieh JM and Wang YC: A synthetic podophyllotoxin derivative exerts anti-cancer effects by inducing mitotic arrest and pro-apoptotic ER stress in lung cancer preclinical models. PLoS One 8: e62082, 2013.
46. Ribeiro IP, Marques F, Barroso L, Rodrigues J, Caramelo F, Melo JB and Carreira IM: Genomic profile of oral squamous cell carcinomas with an adjacent leukoplakia or with an erythroleukoplakia that evolved after the treatment of primary tumor: A report of two cases. Mol Med Rep 16: 6780-6786, 2017.
47. Shin JA, Seo JM, Oh S, Cho SD and Lee KE: Myeloid cell leukemia-1 is a molecular indicator for malignant transformation of oral lichen planus. Oncol Lett 11: 1603-1607, 2016.
48. Nagata M, Wada K, Nakajima A, Nakajima N, Kusayama M, Masuda T, Iida S, Okura M, Kogo M and Kamisaki Y: Role of myeloid cell leukemia-1 in cell growth of squamous cell carcinoma. J Pharmacol Sci 110: 344-353, 2009.
49. Shin JA, Kim JS, Kwon KH, Nam JS, Jung JY, Cho NP and Cho SD: Apoptotic effect of hot water extract of *Sanguisorba officinalis* L. in human oral cancer cells. Oncol Lett 4: 489-494, 2012.
50. Shin JA, Kim JJ, Choi ES, Shim JH, Ryu MH, Kwon KH, Park HM, Seo JY, Lee SY, Lim DW, *et al*: In vitro apoptotic effects of methanol extracts of Dianthus chinensis and Acalypha australis L. targeting specificity protein 1 in human oral cancer cells. Head Neck 35: 992-998, 2013.
51. Choi SJ, Ahn CH, Hong KO, Kim JH, Hong SD, Shin JA and Cho SD: Molecular mechanism underlying the apoptotic modulation by ethanol extract of Pseudolarix kaempferi in mucoepidermoid carcinoma of the salivary glands. Cancer Cell Int 21: 427, 2021.
52. Wertz IE, Kusam S, Lam C, Okamoto T, Sandoval W, Anderson DJ, Helgason E, Ernst JA, Eby M, Liu J, *et al*: Sensitivity to antitubulin chemotherapeutics is regulated by MCL1 and FBW7. Nature 471: 110-114, 2011.
53. Wang W, Wang YQ, Meng T, Yi JM, Huan XJ, Ma LP, Tong LJ, Chen Y, Ding J, Shen JK and Miao ZH: MCL-1 degradation mediated by JNK activation via MEKK1/TAK1-MKK4 contributes to anticancer activity of new tubulin inhibitor MT189. Mol Cancer Ther 13: 1480-1491, 2014.

Copyright © 2023 Yu et al. This work is licensed under a Creative Commons Attribution-NonCommercial-NoDerivatives 4.0 International (CC BY-NC-ND 4.0) License.